

Periplasmic Nitrate Reductase (NapABC Enzyme) Supports Anaerobic Respiration by *Escherichia coli* K-12

Valley Stewart,^{1,2*} Yiran Lu,^{2†} and Andrew J. Darwin^{2‡}

Section of Microbiology, University of California, Davis, California 95616,¹ and Section of Microbiology, Cornell University, Ithaca, New York 14853²

Received 10 September 2001/Accepted 23 November 2001

Periplasmic nitrate reductase (NapABC enzyme) has been characterized from a variety of proteobacteria, especially *Paracoccus pantotrophus*. Whole-genome sequencing of *Escherichia coli* revealed the structural genes *napFDAGHBC*, which encode NapABC enzyme and associated electron transfer components. *E. coli* also expresses two membrane-bound proton-translocating nitrate reductases, encoded by the *narGHJI* and *narZYWW* operons. We measured reduced viologen-dependent nitrate reductase activity in a series of strains with combinations of *nar* and *nap* null alleles. The *napF* operon-encoded nitrate reductase activity was not sensitive to azide, as shown previously for the *P. pantotrophus* NapA enzyme. A strain carrying null alleles of *narG* and *narZ* grew exponentially on glycerol with nitrate as the respiratory oxidant (anaerobic respiration), whereas a strain also carrying a null allele of *napA* did not. By contrast, the presence of *napA*⁺ had no influence on the more rapid growth of *narG*⁺ strains. These results indicate that periplasmic nitrate reductase, like fumarate reductase, can function in anaerobic respiration but does not constitute a site for generating proton motive force. The time course of $\Phi(\textit{napF-lacZ})$ expression during growth in batch culture displayed a complex pattern in response to the dynamic nitrate/nitrite ratio. Our results are consistent with the observation that $\Phi(\textit{napF-lacZ})$ is expressed preferentially at relatively low nitrate concentrations in continuous cultures (H. Wang, C.-P. Tseng, and R. P. Gunsalus, *J. Bacteriol.* 181:5303–5308, 1999). This finding and other considerations support the hypothesis that NapABC enzyme may function in *E. coli* when low nitrate concentrations limit the bioenergetic efficiency of nitrate respiration via NarGHI enzyme.

Nitrate (NO₃⁻), which is relatively abundant in many environments, has three functions in bacterial physiology. Nitrate assimilation provides a source of ammonium for biosynthesis (reviewed in reference 29), nitrate respiration generates proton motive force for energy (reviewed in references 4, 21, and 65), and nitrate dissimilation oxidizes excess reducing equivalents (reviewed in reference 36).

Membrane-bound nitrate reductase (NarGHI enzyme; nitrate reductase A) employs a redox loop to couple quinol oxidation with proton translocation, thereby generating proton motive force for anaerobic respiration. The *Escherichia coli* and *Paracoccus denitrificans* enzymes have been the focus of most biochemical studies (reviewed in references 4, 21, and 65). This enzyme contains Mo-molybdopterin guanine dinucleotide, five iron-sulfur clusters, and diheme cytochrome *b*₅₅₆. NarGHI enzyme activity is inhibited by azide (N₃⁻). Enzyme synthesis is maximally induced during anaerobic growth in the presence of nitrate.

Periplasmic nitrate reductase (NapABC enzyme; nitrate reductase P) also oxidizes quinol, but it is thought that this enzyme is not a coupling site for proton translocation (reviewed in reference 4). Therefore, this enzyme is responsible for nitrate dissimilation. However, periplasmic nitrate reductase can participate indirectly in respiration, by functioning in

an electron transport chain with a proton-translocating enzyme, such as NADH dehydrogenase I (NuoA-N enzyme) (reviewed in references 36 and 45). The *Paracoccus pantotrophus* (*Thiosphaera pantotropha*) enzyme has been the focus of most biochemical studies (reviewed in references 4 and 45). This enzyme contains Mo-molybdopterin guanine dinucleotide, one iron-sulfur cluster, diheme cytochrome *c*₅₅₂ (NapB), and a tetraheme cytochrome *c* (NapC). NapABC enzyme activity is not sensitive to micromolar concentrations of azide.

Periplasmic nitrate reductase of *Paracoccus* spp. is synthesized during aerobic growth irrespective of the added nitrate and is responsible for initiating aerobic denitrification (3). Aerobic nitrate reduction at least in part disposes of excess reductant, because enzyme synthesis is enhanced by growth on highly reduced carbon substrates, such as butyrate (reviewed in reference 45). An analogous role in redox balancing during anaerobic photosynthesis has been suggested for *Rhodobacter* spp. (reviewed in reference 45). Structural genes for the NapABC enzyme and accessory proteins have been characterized for a range of gram-negative bacterial species (reviewed in reference 38).

Systematic sequencing of the *E. coli* K-12 genome revealed a *napFDAGHBC-ccmABCDEF* cluster at centisome 49.5 (7, 25; GenBank accession number U00008). The functions of the conserved NapD protein and the iron-sulfur proteins NapFGH have not been established (reviewed in reference 38). The *ccmABCDEF* genes are required for cytochrome *c* maturation (reviewed in references 22 and 61).

The *E. coli nap-ccm* locus was identified independently in a search for anonymous anaerobically expressed genes (11, 12). Comparison of available sequence data (12; GenBank acces-

* Corresponding author. Mailing address: Section of Microbiology, University of California, One Shields Ave., Davis, CA 95616-8665. Phone: (530) 754-7994. Fax: (530) 752-9014. E-mail: vjstewart@ucdavis.edu.

† Present address: Program in Pharmacology, Graduate School of Medical Sciences of Cornell University, New York, NY 10021.

‡ Present address: Department of Microbiology, New York University School of Medicine, New York, NY 10016.

sion number U00008) revealed that the sequence downstream of the *aeg-46.5* control region corresponds to the 5' end of the *napF* gene. Expression from the *napF* operon promoter requires anaerobiosis, acting through the Fnr protein, and is stimulated by nitrate and nitrite, acting through the Nar regulatory system (11, 12, 16, 18). Subsequent work with *E. coli* has focused on verifying the synthesis and activity of periplasmic nitrate reductase (24, 60; this study), elucidating the transcriptional organization and regulation of the *nap-ccm* complex operon (12, 16, 18, 24, 59, 68), studying the contribution of periplasmic nitrate reductase to anaerobic metabolism (39, 40, 68; this study), and probing the functions of the *ccm* gene products in cytochrome *c* maturation (reviewed in references 22 and 61).

Studies with several denitrifying bacteria, including *P. pantotrophus*, "*Pseudomonas*" sp. strain G-179, and *Rhodobacter sphaeroides* f. sp. *denitrificans*, have demonstrated that periplasmic nitrate reductase can support anaerobic respiration (1, 2, 30). By contrast, studies with *E. coli* have indicated that periplasmic nitrate reductase functions poorly in anaerobic respiration (39, 40). Furthermore, although all organisms have the *napDABC* genes, only denitrifiers carry the *napE* gene, whereas *E. coli* and related ammonifying bacteria carry the *napGH* genes (reviewed in reference 38). This raises the possibility that these accessory genes (or some other aspect of cell physiology) determine whether periplasmic nitrate reductase functions in respiration (in denitrifiers) or simply in dissimilation (in *E. coli*).

Although *E. coli* nitrate respiration has been studied for seven decades (reviewed in reference 53), the *E. coli* NapABC enzyme was first recognized only after whole-genome sequencing. We therefore wished to search for NapA enzyme activity in *E. coli* and to characterize its role in enterobacterial physiology. In this paper we describe an azide-insensitive nitrate reductase activity whose expression requires an intact *nap* locus, in addition to the azide-sensitive activity whose expression requires the *narGHJI* operon. These observations complement the results of independent studies performed in the laboratory of Jeff Cole (24, 59, 60). We also found that periplasmic nitrate reductase supports anaerobic respiration by *E. coli*. Finally, we describe experiments designed to examine the kinetics of *napF* operon expression during growth in batch culture, the results of which complement those of continuous culture studies performed in the laboratory of Rob Gunsalus (68).

(Some of the work presented here was submitted by Marianne T. Shih in 1996 as an undergraduate thesis to the Cornell University Division of Biological Sciences Honors Program.)

MATERIALS AND METHODS

Strains and plasmids. The strains and plasmids used are listed in Table 1 and depicted in Fig. 1. Genetic crosses were performed by P1 *kc*-mediated generalized transduction (34). Standard methods were used for restriction endonuclease digestion, ligation, transformation, and PCR amplification of DNA (32).

Culture media and conditions. Defined, complex, and indicator media for genetic manipulations were used as described previously (32). The antibiotic concentrations were as follows: ampicillin, 200 μ g/ml; chloramphenicol, 25 μ g/ml; kanamycin, 75 μ g/ml; spectinomycin, 100 μ g/ml; streptomycin, 200 μ g/ml; and tetracycline, 20 μ g/ml.

The defined medium used to grow cultures for enzyme assays was buffered with 3-(*N*-morpholino)propanesulfonic acid (MOPS) as previously described (56). The initial pH of this medium is adjusted to 8.0 in order to ameliorate nitrite toxicity (62). Because the pK_a of MOPS is 7.2, the buffering capacity of

this medium continually increases as acidic fermentation products accumulate; at the time of harvest, cultures typically had a pH of about 7.5.

The respiratory oxidants NaNO_3 , NaNO_2 , sodium fumarate, and trimethylamine *N*-oxide were added at concentrations of 40 mM, 5 mM, 50 mM, and 2%, respectively, as indicated below. The carbon sources glucose, glucitol, gluconic acid, mannose, and mannitol were each added at a concentration of 40 mM as indicated below. The carbon source glycerol was added at a concentration of 50 mM along with 0.03% acid-hydrolyzed casein (28). The complex medium used to grow cultures for nitrate reductase assays consisted of one part of MOPS-glucose medium mixed with one part of TY broth (0.8% tryptone, 0.5% yeast extract, 0.5% NaCl) and supplemented with 5 mM NaNO_2 .

Cultures were grown at 37°C. Culture densities were monitored with a Klett-Summerson photoelectric colorimeter (Klett Manufacturing Co., New York, N.Y.) equipped with a no. 66 (red) filter. Anaerobic cultures used for enzyme assays were grown in screw-cap tubes as described previously (56).

Enzyme assays. β -Galactosidase activities were determined at room temperature (approximately 21°C) by monitoring the hydrolysis of *o*-nitrophenyl- β -D-galactoside in CHCl_3 -sodium dodecyl sulfate-permeabilized cells. Specific activities are expressed below in arbitrary units (34). For differential rate plots, the activities are expressed in amounts of orthonitrophenol per milliliter per minute and are not normalized for cell mass (optical density at 600 nm). All cultures were assayed in duplicate, and the values reported below are averages based on at least two independent experiments.

Differential rates of β -galactosidase synthesis (35) were determined for anaerobic cultures essentially as described previously (58). Cultures (25 ml) were continuously bubbled with N_2 - CO_2 (95:5) to maintain anaerobiosis. Samples (1.5 ml) were withdrawn and mixed with 1.5 ml of a solution containing 50 mg of chloramphenicol per ml (to inhibit further protein synthesis) and 1.5 μ l of 50 mM NaN_3 (to inhibit further nitrate reduction). Samples were stored on ice before the assay was performed. The concentration of nitrite in each sample was estimated following reaction with sulfanilic acid (31).

Nitrate reductase activities were determined at room temperature by monitoring the production of nitrite in intact cells (56). Cells were suspended in 0.32 M potassium phosphate (pH 7.1) and stored on ice. Samples (0.8 ml) were mixed with 0.1 ml of a solution containing 0.5 mg of methyl viologen or benzyl viologen per ml. Reactions were started by adding 0.1 ml of a solution containing 4 mg of $\text{Na}_2\text{S}_2\text{O}_4$ per ml, 4 mg of NaHCO_3 per ml, and 0.5 M NaNO_3 . Reactions were terminated by vigorous vortex mixing (to oxidize the viologen), and 1 ml of a sulfanilic acid solution and 1 ml of an *N*-1-naphthylethylenediamine solution were added. Specific activities are expressed below in arbitrary units analogous to Miller units (56). All cultures were assayed in duplicate, and the values reported below are averages based on at least two independent experiments.

Construction of *nap* and *ccm* insertions and deletions. We isolated a series of subclones (Fig. 1) derived from phage 372 (19D1) of the Kohara λ library (27). To construct $\Phi(\textit{nap-lacZ})$ and $\Phi(\textit{ccm-lacZ})$ operon (transcriptional) fusions, each subclone was subjected to insertional mutagenesis with the bacteriophage transposon MudJ (MudI 1734), which forms *lacZ* operon (transcriptional) fusions (9). Several insertions were characterized by restriction mapping and DNA sequence analysis to determine the exact insertion point. Five insertions, spanning the *nap-ccm* region (Fig. 1), were then transplanted into the chromosome by allelic exchange in a *recBC sbcBC* strain (69). The resulting *nap::MudJ* and *ccm::MudJ* insertions were crossed into strain VJS691 and then tested for genetic linkage to a closely linked *narP::Tn10* insertion to confirm their chromosomal location.

The $\Delta\textit{napF1}::\text{Km}$ allele was constructed by cloning a Km^r cassette, liberated by *Pst*I digestion of plasmid pUC4K, between the *Nsi*I sites at position -32 (relative to the transcription initiation site) (12) and at *napF* codon 5. A clone was chosen in which the cassette was oriented with its promoter directed away from the *napF* operon. This insertion was transplanted into the chromosome and tested for linkage as described above for the MudJ insertions.

The *napA4::\Omega*-Cm allele was constructed by cloning the Ω -Cm interposon, liberated by *Bam*HI digestion of plasmid pHP45:: Ω -Cm, into the *Bgl*II site at *napA* codon 578 (7, 25, 60). (The *napA* gene encompasses 828 codons.) This insertion was transplanted into the chromosome by integration-excision allelic exchange (51), with selection for Cm^r Sm^r segregants (plasmid-free segregants were selected as Sm^r constructs after loss of the dominant *rpsL*⁺ Sm^s allele). We then used generalized transduction to construct *napA4::\Omega*-Cm *nap::MudJ* and *napA4::\Omega*-Cm *ccm::MudJ* double mutants. The resulting strains were subjected to transduction-mediated three-point crosses, employing flanking *Tn10* (Tc^r) insertions, to confirm the genetic map order of the MudJ (Km^r) and Ω -Cm elements in each strain (data not shown).

The $\Delta\textit{napA5}$ deletion was constructed by loop deletion mutagenesis (70) by using the following mutagenic oligonucleotide complementary to an internal segment of the *napA* gene coding strand: 5'-ACTGCCGGTGTGCCAGTGCTCGAGA

TABLE 1. Strains and plasmids

Strain or plasmid	Genotype	Reference or source
<i>Escherichia coli</i> K-12 strains		
BW18812	$\Delta(lacI-codB)X74 \Delta phoA532 \Delta uidA \Delta phn$	33
LCB2048	<i>thi-1 thr-1 leu-6 lacY1 supE44 rpsL175</i> $\Delta(narGH)::Km \Delta(narUZ)::\Omega$ -Sp	6
POI1734	Mu dII1734 <i>ara::(Mu cts)3</i> $\Delta(lac-proAB)X111 rpsL$	9
RK4353	<i>araD139</i> $\Delta(argF-lac)U169 flhD5301 gyrA129 non-9 rpsL150 ptsF25 relA1 deoC1$	55
RK5268	Like RK4353 but <i>narG205::Tn10</i>	55
VJS632	Prototroph	56
VJS676	Like VJS632 but $\Delta(argF-lac)U169$	56
VJS691	Like VJS632 but $\Delta(argF-lac)U169 \Delta(trpEA)2$	56
VJS2197	Like VJS676 but $\lambda\Phi(narG-lacZ)$	43
VJS2430	Like VJS676 but $\lambda\Phi(narG-lacZ) \Delta narX242 zch-2084::\Omega$ -Cm	43
VJS3040	Like VJS676 but $\lambda\Phi(narG-lacZ) narQ251::Tn10d(Tc)$	43
VJS3861	Like VJS676 but $\lambda\Phi(nrfA-lacZ)$	This study
VJS4734	Like VJS676 but $\lambda\Phi(napF-lacZ) [\Delta-275]$	16
VJS4799	Like VJS676 but $\lambda\Phi(napF-lacZ) [\Delta-275] narL215::Tn10$	16
VJS5432	Like VJS691 but $\Delta(narUZ)::\Omega$ -Sp	This study
VJS5433	Like VJS691 but $\Delta(narUZ)::\Omega$ -Sp $\Delta napF1::Km$	This study
VJS5435	Like VJS691 but <i>narG205::Tn10</i> $\Delta napF1::Km$	This study
VJS5436	Like VJS691 but <i>narG205::Tn10</i> $\Delta(narUZ)::\Omega$ -Sp	This study
VJS5437	Like VJS691 but <i>narG205::Tn10</i> $\Delta(narUZ)::\Omega$ -Sp $\Delta napF1::Km$	This study
VJS5917	Like VJS6737 but $\Delta(narUZ)::\Omega$ -Sp	This study
VJS5918	Like VJS6737 but $\Delta(narUZ)::\Omega$ -Sp $\Delta napA5$	This study
VJS5919	Like VJS6737 but $\Delta(narUZ)::\Omega$ -Sp <i>narG205::Tn10</i>	This study
VJS5920	Like VJS6737 but $\Delta(narUZ)::\Omega$ -Sp <i>narG205::Tn10</i> $\Delta napA5$	This study
VJS6737	Like BW18812 but <i>rpsL150</i>	This study
Plasmids		
pHG165	Ap ^r , pUC8 polylinker, medium-copy-number cloning vector	52
pHP45:: Ω -Cm	Ap ^r Cm ^r , source of Ω -Cm interposon	20
pKAS46	Ap ^r Km ^r <i>rpsL</i> ⁺ , allelic-exchange vector	51
pKT53	Tc ^r , source of <i>nrfA</i> control region	64
pRS415	Ap ^r , <i>lacZ</i> operon fusion vector	50
pUC4K	Ap ^r Km ^r , source of Km ^r (<i>aph</i>) cassette	66
pVJS1510	Ap ^r <i>napFDA</i> ⁺ , 2.9-kb <i>PstI</i> - <i>Bgl</i> III insert in pHG165 ^a	This study
pVJS1521	Ap ^r Km ^r , $\Delta napF1::Km$ in pVJS1510	This study
pVJS1725	Ap ^r Cm ^r Km ^r , <i>napA4::\Omega</i> -Cm in pVJS1729	This study
pVJS1728	Ap ^r Km ^r , $\Delta napA5$ in pVJS1729	This study
pVJS1729	Ap ^r Km ^r <i>nap'AGHBC-ccmA'</i> , 5.5-kb <i>NotI</i> - <i>Bam</i> HI insert in pKAS46 ^a	This study

^a See Fig. 1.

TCCGATTTTCGCTTCGCC (the underlined *XhoI* site corresponds to the complement of the Glu-723 and Leu-559 codons). Thus, the deletion removed 163 codons (codons 560 through 722), including the *Bgl*III site at codon 578, while simultaneously introducing a new *XhoI* site.

The $\Delta napA5$ allele was transplanted into the chromosome (51) of a $\Phi(napA-uidA)$ derivative of strain VJS6737, in which a *uidA* cassette (33) was inserted into the *Bgl*III site at *napF* codon 578 (V. Stewart and J. Shi, unpublished data). Sm^r segregants were isolated on agar containing the UidA indicator X-Gluc (5-bromo-4-chloro-3-indolyl- β -D-glucuronide) to facilitate identification of UidA⁻ strains in which the $\Delta napA5$ allele had replaced the resident *napA::uidA* allele. The presence of the deletion was confirmed by whole-colony PCR analysis (70), in which primers flanking the site of the deletion were used and the presence of the introduced *XhoI* site was examined.

Construction of a $\Phi(nrfA-lacZ)$ gene (translational) fusion. The *nrfA* operon control region from position -209 to position 131 (relative to the transcription initiation site) was subcloned as an *EcoRI*-*Hind*III fragment (64) into a polylinker plasmid to place a *Bam*HI site adjacent to the *Hind*III site. The resulting *EcoRI*-*Bam*HI fragment was then cloned into plasmid pRS414 (50) to form a plasmid-borne $\Phi(nrfA-lacZ)$ gene (translational) fusion. The fusion construct was crossed into bacteriophage λ RS45 (50), and monocopy lysogens were identified by a whole-colony PCR test (41). Similarly constructed $\lambda\Phi(narG-lacZ)$ gene and $\lambda\Phi(napF-lacZ)$ operon fusions have been described previously (16, 42).

RESULTS AND DISCUSSION

***E. coli* periplasmic nitrate reductase.** *E. coli* contains three sets of nitrate reductase genes: the *narGHJI* operon, encoding the membrane-bound NarGHI enzyme; the homologous *narZYWV* operon, encoding the membrane-bound NarZYV en-

zyme; and the *napFDAGHBC* operon, encoding the periplasmic NapABC enzyme. In order to distinguish the different activities, we used generalized transduction to construct a series of isogenic strains with all combinations of *nar* and *nap* polar null lesions. The defined null alleles *narG205::Tn10* (55) and $\Delta(narUZ)::\Omega$ -Sp (6) were available, so we fabricated $\Delta napF1::Km$, in which the *napF* operon promoter control region and the 5' end of the *napF* gene were replaced with a Km^r cassette (see Materials and Methods).

Strains were grown anaerobically with nitrite, which in batch culture induces high-level *napF* operon expression (24, 43, 68). Reduced viologen-linked nitrate reductase activity was measured in whole cells as described in Materials and Methods. The most reproducible results were obtained in assays performed with unbroken freshly cultured cells, suggesting that NapA activity may be relatively unstable (NarG activity is quite stable). Instability was also noted by Thomas et al. (60).

Results are shown in Table 2. The NarZYV enzyme contributed little to the overall nitrate reductase activity (compare the activities of strains VJS5435 and VJS5437), as expected since low levels of this enzyme are synthesized during exponential growth (10). The NarG⁺ NapA⁺ strain VJS5432 exhibited significant endogenous activity, which increased four- to fivefold when reduced viologen was provided as an artificial electron donor. The NarG⁺ NapA⁻ strain VJS5433 exhibited

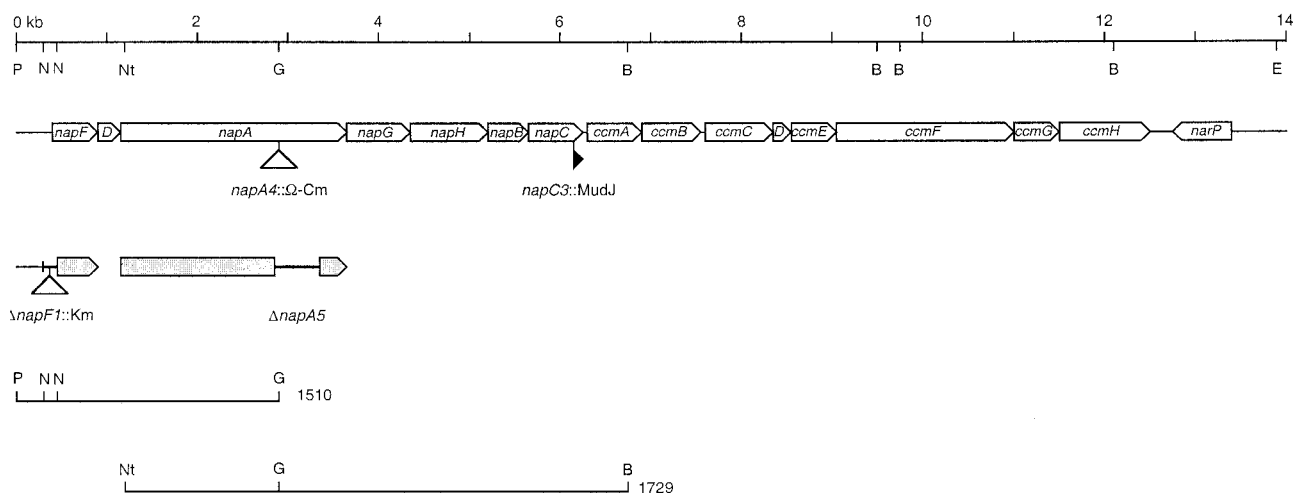


FIG. 1. *nap-ccm* cluster. The seven *nap* genes, eight *ccm* genes, and the convergently transcribed *narP* gene are depicted to scale as open arrows. Insertions of MudJ and Ω -Cm are indicated by solid and open triangles, respectively. The deletion-substitution $\Delta napF1::Km$ and the deletion $\Delta napA5$ are indicated by thick lines with gray arrows. The restriction endonuclease sites indicated are *Bam*HI (B), *Bgl*III (G), *Eco*RI (E), *Not*I (Nt), *Nsi*I (N), and *Pst*I (P) sites. Only two of seven *Nsi*I sites used to construct the $\Delta napF1::Km$ allele are shown. The inserts for pVJS subclones listed in Table 1 are shown.

approximately 80% of the $NarG^+ NapA^+$ viologen-stimulated activity, whereas the $NarG^- NapA^+$ strain VJS5436 exhibited 15 to 30% of the $NarG^+ NapA^+$ viologen-stimulated activity and very little endogenous (viologen-independent) activity.

Previously characterized NapA enzymes are not sensitive to azide, in contrast to NarG enzyme (reviewed in references 4 and 21). Our results (Table 2) revealed that activity of the $NarG^+ NapA^-$ strain VJS5433 was inhibited 8- to 10-fold by azide, whereas activity of the $NarG^- NapA^+$ strain was not sensitive to azide. These results established that an azide-insensitive nitrate reductase activity is present in *E. coli* and that this activity requires an intact *napF* operon.

Grove et al. employed activity staining of native gels to detect nitrate reductase activity in the periplasmic fraction of a *narG* null strain, and this activity was not present in extracts of a *nap* null strain (23). These authors also presented evidence that *napB* and *napC* encode Nap-associated cytochromes *c*. Subsequently, Thomas et al. determined the amino-terminal sequences of the NapA and NapB proteins, confirming the structural gene assignments (60). These results, together with those presented above, demonstrate that *E. coli* synthesizes a periplasmic azide-insensitive NapABC enzyme that is homologous to enzymes characterized in other bacteria (reviewed in reference 4).

Potter et al. detected only very low levels of NapA activity when reduced methyl viologen was used as the electron donor in broken cells, yet they detected significant levels of activity when formate or glycerol was used as the electron donor in whole cells (40). In our viologen-dependent assay, which detected substantial levels of NapA activity (Table 2), we used freshly harvested whole cells.

Function of *E. coli* periplasmic nitrate reductase. We sought culture conditions under which the presence of the NapABC enzyme would result in a clear phenotype. Therefore, we constructed an in-frame deletion in the *napA* gene in order to eliminate Nap enzyme activity while avoiding polarity on *ccm* gene expression (since respiratory nitrite reductase requires the Ccm^+ function for activity). The $\Delta napA5$ deletion (Fig. 1)

was constructed and transplanted into the chromosome as described in Materials and Methods.

To determine whether the $\Delta napA5$ deletion was polar on downstream gene expression, we monitored β -galactosidase expression in strains carrying the downstream *napC3::MudJ* insertion (Fig. 1). Strains carrying *napC3::MudJ* in combination with *napA^+*, *napA4::Ω-Cm*, or $\Delta napA5$ were cultured anaerobically in MOPS-glucose medium with and without nitrite, and β -galactosidase activities were measured. The *napA^+* strain exhibited approximately 20-fold induction of $\Phi(napC-lacZ)$ expression by nitrite. A similar level of nitrite-induced $\Phi(napC-lacZ)$ expression was observed in the $\Delta napA5$ strain. By contrast, the *napA::Ω-Cm* insertion significantly reduced $\Phi(napC-lacZ)$ expression due to strong transcriptional polarity. We concluded that the $\Delta napA5$ allele exerts no significant polarity on downstream *nap-ccm* gene expression.

Isogenic strains carrying *narG^+* or *narG205::Tn10* in combination with *napA^+* or $\Delta napA5$ were batch cultured anaerobically in MOPS-glycerol-casein medium supplemented with nitrate or fumarate as described in Materials and Methods.

TABLE 2. Nitrate reductase activities of $NarG^-$, $NapA^-$, and $NarZ^-$ strains

Strain	Phenotype			Nitrate reductase sp act with the following electron donors ^a :				
				None, without N_3^-		Methyl viologen		Benzyl viologen
	NarG	NapA	NarZ	Without N_3^-	With N_3^-	Without N_3^-	With N_3^-	
VJS5432	+	+	-	86	330	190	480	250
VJS5433	+	-	-	96	260	27	400	25
VJS5436	-	+	-	4	97	130	73	52
VJS5435	-	-	+	<1	2	2	<1	<1
VJS5437	-	-	-	<1	<1	<1	<1	<1

^a Specific activities were determined as described in Materials and Methods and are expressed in arbitrary units. Assays were performed with different dithionite-reduced electron donors. Azide (50 μ M) was added to some preparations.

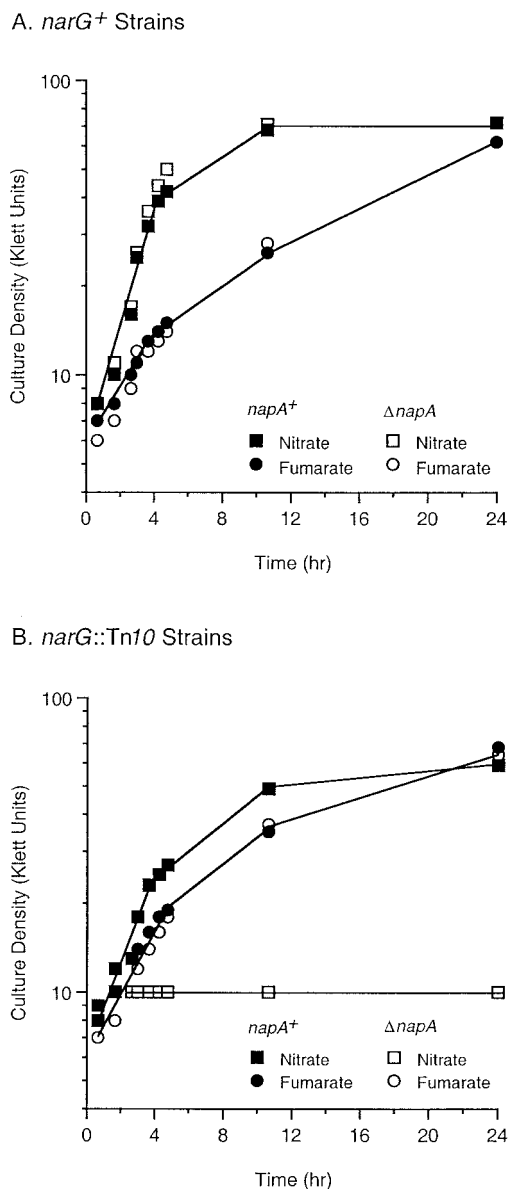


FIG. 2. Anaerobic respiration: growth curves for anaerobic cultures in MOPS-glycerol-acid-hydrolyzed casein medium supplemented with nitrate or fumarate as the respiratory oxidant. (A) Data for the *narG*⁺ strains VJS5917 (*napA*⁺) and VJS5918 ($\Delta napA5$). (B) Data for the *narG*::Tn10 strains VJS5919 (*napA*⁺) and VJS5920 ($\Delta napA5$). All strains carry $\Delta(narUZ)::\Omega$ -Sp.

(Anaerobic growth with glycerol requires respiration with a terminal oxidant, which in this case was either nitrate or fumarate.) The *narG*⁺ strain grew on nitrate with an early-exponential-phase doubling time of about 85 min irrespective of the presence of *napA*⁺ (Fig. 2A). By contrast, the *narG*::Tn10 *napA*⁺ strain grew on nitrate (early-exponential-phase doubling time, about 150 min) only slightly faster than on fumarate (early-exponential-phase doubling time, about 165 min) (Fig. 2B). Strikingly, the *narG*::Tn10 $\Delta napA$ double mutant did not grow with nitrate as the electron acceptor. All four strains had equivalent growth rates on fumarate.

These results demonstrate that *E. coli* can use periplasmic

nitrate reductase and fumarate reductase equally well in a respiratory chain involving glycerol 3-phosphate oxidation. Fumarate reductase itself does not constitute a coupling site for generating proton motive force from quinol oxidation (63; reviewed in references 21 and 65). Therefore, the observed growth phenotypes support the conclusion that periplasmic nitrate reductase is not a coupling site (4, 36). These observations do not eliminate the formal possibility that periplasmic nitrate reductase simply provides nitrite as the substrate for periplasmic nitrite reductase (NrfABCD enzyme), which is known to support anaerobic respiration (reviewed in references 5 and 21). However, expression of the *nrfABCDEFG* operon is strongly inhibited by nitrate (64) (see Fig. 6). Therefore, the most economical hypothesis is that *E. coli* periplasmic nitrate reductase functions directly to support anaerobic respiration.

Studies with a *P. pantotrophus* double mutant carrying a null allele of *narH* in addition to an operator-constitutive mutation in the *napE* operon control region (49) revealed that periplasmic nitrate reductase can support anaerobic respiration on nitrate with about one-third the wild-type doubling time (2). By contrast, however, an *E. coli narG narZ* double-null *nap*⁺ strain grew only arithmetically in defined glycerol-casein medium supplemented with 20 mM nitrate (39). Subsequent work indicated that this growth defect was partially suppressed by introduction of a *narL* null allele (40). Strains derived from both the MC4100 (RK4353) and C600 (LCB320) lineages exhibited this phenotype. The authors of those studies concluded that NarL antagonism of *napF* operon expression (16) caused the growth defect on nitrate.

By contrast, we observed robust exponential growth with strains derived from both the BD792 (BW18812) and RK4353 lineages (Fig. 2 and data not shown). We used $\lambda\Phi(narG-lacZ)$ specialized transducing phage to confirm that the strains which we used harbored *narL*⁺ alleles (54). We note that $\Phi(napF-lacZ)$ expression during batch culture of *narL*⁺ strains is induced about 10-fold by nitrate, compared to the approximately 20-fold induction by nitrite (16, 68). Thus, the inhibitory effect of NarL and nitrate is relatively minor compared to the overall induction of $\Phi(napF-lacZ)$ expression.

Carbon source oxidation state does not regulate *napF* operon expression. In *P. pantotrophus*, *P. denitrificans*, and *Rhodobacter capsulatus*, growth on reduced carbon sources results in increased NapABC synthesis compared to the synthesis observed when the organisms are grown on oxidized carbon sources (46, 47, 49). This reflects the enzyme's role in these organisms in maintaining redox balance (nitrate dissimilation) even in aerated cultures. We therefore batch cultured the *nar*⁺ *nap*⁺ $\lambda\Phi(napF-lacZ)$ strain VJS4734 anaerobically in MOPS-nitrite medium supplemented with carbon sources having different oxidation states. However, the relative levels of $\Phi(napF-lacZ)$ expression in mid-exponential-phase cultures differed less than twofold, and the small variations observed did not reflect the relative oxidation states of the carbon sources (data not shown). Expression was slightly higher in the culture grown with glucitol (more reduced) than in the culture grown with glucose or glucuronic acid (more oxidized). Conversely, expression was slightly higher in the culture grown with mannose (more oxidized) than in the culture grown with mannitol (more reduced). Indeed, the patterns were more reminiscent of catabolite repression, as glucose and mannitol are more effective

elicitors of catabolite repression than glucitol and mannose are (37). Thus, at least for the carbon sources tested, we observed no effect of oxidation state on $\Phi(\text{napF-lacZ})$ expression.

Differential regulation by nitrate and nitrite: kinetics of $\Phi(\text{napF-lacZ})$ induction. Our previous conclusions regarding expression of the *napF*, *narG*, and other Nar-regulated operons were based on measurements obtained for mid-exponential-phase batch cultures started with either 40 mM nitrate or 5 mM nitrite. Because growing cultures quickly consume nitrate, we use an excess to ensure that saturating (millimolar) concentrations were present at the time of harvest. The concentration of nitrite employed is sufficient to observe regulated gene expression without inhibiting growth rates and yields (see also Materials and Methods). Thus, these cultures allow us to draw conclusions regarding differential responses to saturating concentrations of the structurally related signals nitrate and nitrite. They do not allow us to draw conclusions regarding responses to limiting concentrations of these compounds (68).

Cognizant of these limitations of batch culture analysis, we hypothesized that the *napF* promoter might be more efficiently expressed during growth with a limiting concentration of nitrate. We therefore examined the kinetics of $\Phi(\text{napF-lacZ})$ induction in response to different nitrate concentrations. Two parallel batch cultures of the *nar⁺ nap⁺ $\lambda\Phi(\text{napF-lacZ})$* strain VJS4734 were grown to the early exponential phase in MOPS-glucose medium. Nitrate was added to a final concentration of 1 mM to one culture and to a final concentration of 10 mM to the other. Samples were withdrawn and used to measure β -galactosidase activity and nitrite concentration (see Materials and Methods), and the results were analyzed by constructing differential rate plots (26, 35). We observed no difference in the initial rates of β -galactosidase synthesis in the two cultures (data not shown).

We next investigated the effects of nitrate versus the effects of nitrite. Two parallel cultures were grown to the early exponential phase. Nitrate was added to a final concentration of 10 mM to one culture, and nitrite was added to a final concentration of 1 mM to the other. Samples were withdrawn and used to measure β -galactosidase activity and nitrite concentration. The results are shown in Fig. 3. The nitrite-induced culture steadily consumed nitrite, whereas the nitrate-induced culture rapidly accumulated nitrite. Again, the initial rates of $\Phi(\text{napF-lacZ})$ expression were the same in both cultures for about one-half a generation (Fig. 3). Therefore, the initial rates of $\Phi(\text{napF-lacZ})$ expression were the same upon induction with 1 mM nitrate, 10 mM nitrate, and 1 mM nitrite.

Differential regulation by nitrate and nitrite: time course of $\Phi(\text{napF-lacZ})$ expression. Although the initial rates of enzyme synthesis were indistinguishable, we observed that the rates in the cultures supplemented with 10 mM nitrate began to fluctuate within 1 doubling time (not shown in Fig. 3). We reasoned that the decrease observed was due to NarL-mediated antagonism (16). To test this hypothesis, we monitored the differential rates of $\Phi(\text{napF-lacZ})$ expression in both *narL⁺* and *narL::Tn10* strains grown in batch cultures started with 5 mM nitrate (Fig. 4). This experiment differed from those described above because nitrate was present from the beginning of growth. In this experiment, we were concerned with the patterns of gene expression as nitrate was depleted from the

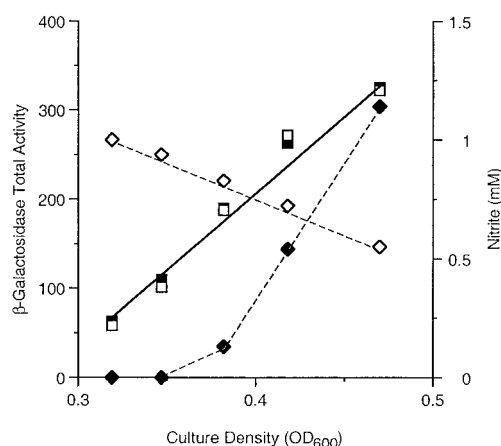


FIG. 3. Differential rates of $\Phi(\text{napF-lacZ})$ induction. Duplicate cultures of strain VJS4734 were grown anaerobically in MOPS-glucose medium. At the early exponential phase, nitrate (solid symbols) and nitrite (open symbols) were added to final concentrations of 10 and 1 mM, respectively. Samples were withdrawn and assayed for total β -galactosidase activity (■ and □) and nitrite concentration (◆ and ◇). OD₆₀₀, optical density at 600 nm.

medium rather than with the initial rates of synthesis when nitrate was added.

Figure 4A shows a representative growth curve for the *nar⁺ nap⁺ $\lambda\Phi(\text{napF-lacZ})$* strain VJS4734. At each time point, a sample was withdrawn and assayed for β -galactosidase activity and for nitrite concentration as described in Materials and Methods. Nitrite, formed by the action of nitrate reductase, accumulated nearly quantitatively and was then consumed by the action of nitrite reductase (forming ammonium). This pattern of nitrite accumulation and consumption was previously noted by DeMoss and Hsu (19). Thus, we were able to monitor the effects on gene expression of continually changing ratios of the two signal ligands.

In the *narL⁺* strain, the rate of $\Phi(\text{napF-lacZ})$ expression exhibited a complex pattern. The rate seemed to increase about twofold as the nitrite concentration peaked (i.e., at about the time that the nitrate in the culture medium was exhausted) (Fig. 4B and data not shown). This is consistent with the conclusion of Wang et al. (68), drawn from studies of continuous cultures, that $\Phi(\text{napF-lacZ})$ expression is maximal at submillimolar concentrations of nitrate. As nitrite was rapidly consumed, β -galactosidase synthesis transiently stopped and then resumed. Finally, when the nitrite in the culture medium was exhausted, synthesis again stopped (Fig. 4B and data not shown).

In striking contrast, the *narL* null strain exhibited a steady rate of $\Phi(\text{napF-lacZ})$ expression that was not affected by changes in the nitrate/nitrite ratio; synthesis stopped only after the nitrite was exhausted (Fig. 4B and data not shown). Thus, the complex pattern of $\Phi(\text{napF-lacZ})$ expression in the *narL⁺* strain evidently reflected antagonism by phospho-NarL, which competes with the activator phospho-NarP for a common DNA binding site upstream of the *napF* operon promoter (16, 18). These experiments, together with complementary studies of continuous cultures (68), revealed that the levels of $\Phi(\text{napF-lacZ})$ expression observed in batch cultures provide only one view of the complexity that underlies transcriptional regulation of the *napF* promoter.

A. Growth Curve

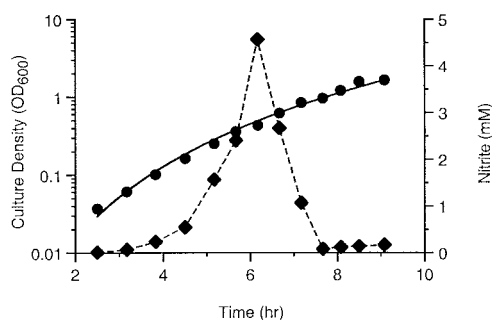
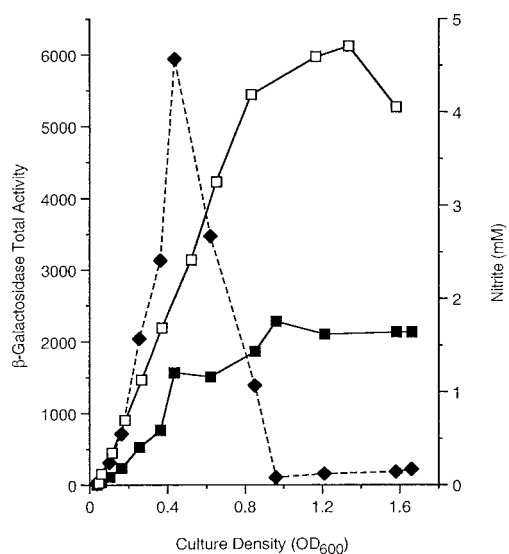
B. $\Phi(\text{napF-lacZ})$ Expression

FIG. 4. Differential rates of $\Phi(\text{napF-lacZ})$ expression. Cultures of the $\lambda\Phi(\text{napF-lacZ})$ strains VJS4734 (narL^+) and VJS4799 ($\text{narL}::\text{Tn10}$) were grown anaerobically in MOPS-glucose medium supplemented with 5 mM nitrate. (A) Growth curve (●) and nitrite concentrations (◆) for strain VJS4734. This pattern was typical for strains used in this experiment and in the experiments whose results are shown in Fig. 5 and 6. (B) Total β -galactosidase activities in cultures of strains VJS4734 (■) and VJS4799 (□) and, for reference, nitrite concentrations in the culture of strain VJS4734 (◆). OD_{600} , optical density at 600 nm.

In continuous culture, $\Phi(\text{napF-lacZ})$ expression was maximal at a relatively low concentration of nitrate, about 0.5 mM (68). Consistent with this, the time course experiments revealed that $\Phi(\text{napF-lacZ})$ expression seemed to increase as nitrate was removed from the medium (Fig. 4B and data not shown). By contrast, maximal $\Phi(\text{narG-lacZ})$ expression in continuous culture requires more than 5 mM nitrate. It was hypothesized that this pattern of regulation reflects a relatively low K_m for nitrate of periplasmic nitrate reductase compared to the K_m for nitrate of the membrane-bound enzyme (68). Arguing against this notion, studies of *Paracoccus* sp. enzymes in which reduced methyl viologen was used as the electron donor revealed that the K_m for nitrate of NarGHI enzyme was more than fourfold lower than the K_m for nitrate of NapAB enzyme (0.28 versus 1.3 mM) (8, 14). However, we note that the K_m of NarGHI enzyme was 20-fold lower in assays in which

a more physiologically relevant quinol analog was used as the electron donor (14); analogous studies with NapABC-NapFGH enzyme have not been described.

We suggest an alternative hypothesis to explain why periplasmic nitrate reductase might be preferentially expressed during growth in the presence of low nitrate concentrations. For nitrate respiration, which is mediated by NarGHI enzyme, nitrate must be imported to the cytoplasm; for nitrite respiration, which is mediated by NrfABC enzyme, the resultant nitrite must be exported back to the periplasm (19, 48). In the presence of excess nitrate, the energy cost for this transport would likely be more than supplanted by an NarGHI-generated proton motive force. When nitrate is limiting, however, it may be more economical to simply reduce nitrate in the periplasm (concomitant with oxidation of reducing equivalents) and deliver it directly to the periplasmic respiratory nitrite reductase (13).

Differential regulation by nitrate and nitrite: time course of $\Phi(\text{narG-lacZ})$ and $\Phi(\text{nrfA-lacZ})$ expression. Because of the complex pattern for $\Phi(\text{napF-lacZ})$ expression described above, we examined the synthesis patterns for other Nar-regulated structural genes, including those for the membrane-bound nitrate reductase (*narGHJ* operon), the nitrate-inducible formate dehydrogenase (*fdnGHI* operon), and the periplasmic respiratory nitrite reductase (*nrfA-G* operon).

Studies performed with batch cultures have shown that induction of $\Phi(\text{narG-lacZ})$ expression is maximal during anaerobic growth with nitrate and much weaker during growth with nitrite (43, 44, 68). Analysis of continuous cultures yielded the same results (68). Thus, we monitored the differential rates of $\Phi(\text{narG-lacZ})$ expression in nar^+ , ΔnarX , and $\text{narQ}::\text{Tn10}$ strains grown in batch cultures started with 5 mM nitrate, as

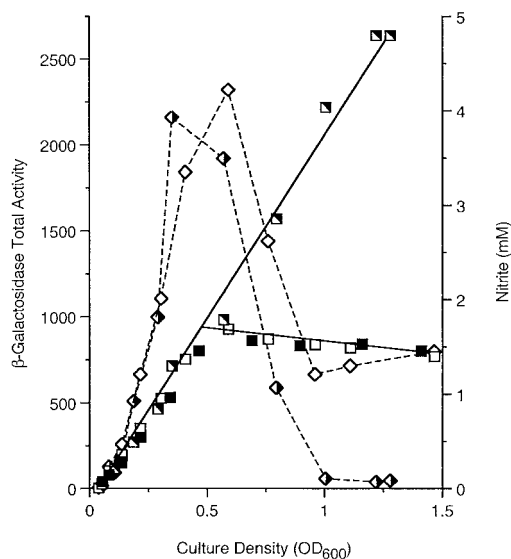


FIG. 5. Differential rates of $\Phi(\text{narG-lacZ})$ expression. Cultures of the $\lambda\Phi(\text{narG-lacZ})$ strains VJS2197 (nar^+) (solid symbols), VJS2430 ($\Delta\text{narX narQ}^+$) (half-open symbols), and VJS3040 ($\text{narX}^+ \text{narQ}::\text{Tn10}$) (open symbols) were grown anaerobically in MOPS-glucose medium supplemented with 5 mM nitrate. Samples were withdrawn and assayed for total β -galactosidase activity (squares) and nitrite concentration (diamonds). The values for nitrite concentration in the culture of strain VJS2197 are omitted for clarity. OD_{600} , optical density at 600 nm.

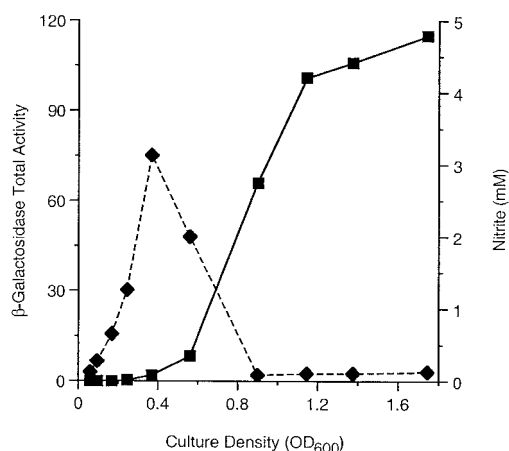


FIG. 6. Differential rate of $\Phi(nrfA-lacZ)$ expression. A culture of the $\lambda\Phi(nrfA-lacZ)$ strain VJS3861 was grown anaerobically in MOPS-glucose medium supplemented with 5 mM nitrate. Samples were withdrawn and assayed for total β -galactosidase activity (■) and nitrite concentration (◆). OD₆₀₀, optical density at 600 nm.

described above (Fig. 5). (The cultures of the nar^+ and $\Delta narX$ strains exhibited similar patterns of nitrite accumulation and consumption; for clarity, Fig. 5 shows only the data for the $\Delta narX$ strain.)

Enzyme synthesis in the nar^+ strain proceeded at a steady rate until the nitrite concentration peaked (i.e., until about the time that the nitrate in the culture medium was exhausted), and then synthesis stopped. The pattern of $\Phi(fdnG-lacZ)$ expression in a nar^+ strain was virtually identical (data not shown), as expected (43). Expression of $\Phi(narG-lacZ)$ in the $narQ$ null strain was likewise indistinguishable. By contrast, $\Phi(narG-lacZ)$ expression in the $narX$ null strain continued unabated (Fig. 5). This is consistent with the postulated function of the NarX protein as a negative regulator (cophosphatase) of phospho-NarL function (reviewed in references 15 and 57) and suggests that this activity has a physiological role (namely, shutoff of target gene expression upon nitrate depletion). Thus, previous conclusions resulting from studies of mid-exponential-phase batch cultures are concordant with the results of these time course experiments.

We note in passing that the culture of the $narQ$ null strain did not consume nitrite when it was present at a concentration below about 1 mM (Fig. 5), implying that at least one gene required for high-affinity nitrite uptake or reduction requires $narQ^+$ for expression. We have not pursued this observation.

Studies with both batch and continuous cultures show that $\Phi(nrfA-lacZ)$ expression and $\Phi(narG-lacZ)$ expression are regulated reciprocally; $\Phi(nrfA-lacZ)$ expression is inhibited during anaerobic growth with nitrate and induced during growth with nitrite (17, 43, 64, 67). Thus, we monitored the differential rate of $\Phi(nrfA-lacZ)$ expression in a nar^+ strain grown in a batch culture started with 5 mM nitrate (Fig. 6). Enzyme synthesis proceeded at a very low rate until the nitrite concentration peaked (i.e., until about the time that the nitrate in the culture medium was exhausted), and then the rate of synthesis was steady and high until the nitrite was exhausted. Again, the results of these time course experiments are completely consistent with previous conclusions.

Thus, in contrast to the complex patterns of $\Phi(napF-lacZ)$ expression described above, the patterns of $\Phi(narG-lacZ)$, $\Phi(fdnG-lacZ)$, and $\Phi(nrfA-lacZ)$ expression were simple and readily interpretable.

Epilogue. Studies of *E. coli* periplasmic nitrate reductase have continually challenged our view of this organism's physiology. In the context of regulated gene expression, the *napF* operon control region is unique among known Nar-regulated targets in both its architecture and its response to the transcriptional regulators NarL and NarP. These unique features evidently underlie uniquely complex patterns of transcriptional regulation. Continued acceptance of the challenges presented should reveal additional, perhaps subtle aspects of the Nar regulatory network.

ACKNOWLEDGMENTS

We are grateful to Jiarong Shi (Cornell University) and to Janine Lin and Chesi Ho (University of California, Davis) for their efforts in evaluating the $\Delta napA5$ strains. We thank Francisco Blasco, Malcolm Casadaban, Joachim Fellay, Robert Simons, Karen Skorupski, the late Gordon Stewart, Kerry Tyson, and Barry Wanner for generous gifts of strains and plasmids.

This study was supported by Public Health Service grant GM36877 from the National Institute of General Medical Science.

REFERENCES

1. Bedzyk, L., T. Wang, and R. W. Ye. 1999. The periplasmic nitrate reductase in *Pseudomonas* sp. strain G-179 catalyzes the first step of denitrification. *J. Bacteriol.* **181**:2802–2806.
2. Bell, L. C., M. D. Page, B. C. Berks, D. J. Richardson, and S. J. Ferguson. 1993. Insertion of transposon Tn 5 into a structural gene of the membrane-bound nitrate reductase of *Thiosphaera pantotropha* results in anaerobic overexpression of periplasmic nitrate reductase activity. *J. Gen. Microbiol.* **139**:3205–3214.
3. Bell, L. C., D. J. Richardson, and S. J. Ferguson. 1990. Periplasmic and membrane-bound nitrate reductases in *Thiosphaera pantotropha*: the periplasmic enzyme catalyzes the first step in aerobic denitrification. *FEBS Lett.* **265**:85–87.
4. Berks, B. C., S. J. Ferguson, J. W. B. Moir, and D. J. Richardson. 1995. Enzymes and associated electron transport systems that catalyze the respiratory reduction of nitrogen oxides and oxyanions. *Biochim. Biophys. Acta* **1232**:97–173.
5. Berks, B. C., D. J. Richardson, C. Robinson, A. Reilly, R. T. Aplin, and S. J. Ferguson. 1994. Purification and characterization of the periplasmic nitrate reductase from *Thiosphaera pantotropha*. *Eur. J. Biochem.* **220**:117–124.
6. Blasco, F., F. Nunzi, J. Pommier, R. Brasseur, M. Chippaux, and G. Giordano. 1992. Formation of active heterologous nitrate reductases between nitrate reductases A and Z of *Escherichia coli*. *Mol. Microbiol.* **6**:209–219.
7. Blattner, F. R., G. Plunkett, C. A. Bloch, N. T. Perna, V. Burland, M. Riley, J. Collado-Vides, J. D. Glasner, C. K. Rode, G. F. Mayhew, J. Gregor, N. W. Davis, H. A. Kirkpatrick, M. A. Goeden, D. J. Rose, B. Mau, and Y. Shao. 1997. The complete genome sequence of *Escherichia coli* K-12. *Science* **277**:1453–1462.
8. Butler, C. S., J. M. Charnock, B. Bennett, H. J. Sears, A. J. Reilly, S. J. Ferguson, C. D. Garner, D. J. Lowe, A. J. Thomson, B. C. Berks, and D. J. Richardson. 1999. Models for molybdenum coordination during the catalytic cycle of periplasmic nitrate reductase from *Paracoccus denitrificans* derived from EPR and EXAFS spectroscopy. *Biochemistry* **38**:9000–9012.
9. Castillo, B. A., P. Olfson, and M. J. Casadaban. 1984. Plasmid insertion mutagenesis and *lac* gene fusion with mini-Mu bacteriophage transposons. *J. Bacteriol.* **158**:488–495.
10. Chang, L., L. I. Wei, J. P. Audia, R. A. Morton, and H. E. Schellhorn. 1999. Expression of the *Escherichia coli* NRZ nitrate reductase is highly growth phase dependent and is controlled by RpoS, the alternative vegetative sigma factor. *Mol. Microbiol.* **34**:756–766.
11. Choe, M., and W. S. Reznikoff. 1991. Anaerobically expressed *Escherichia coli* genes identified by operon fusion techniques. *J. Bacteriol.* **173**:6139–6146.
12. Choe, M., and W. S. Reznikoff. 1993. Identification of the regulatory sequence of anaerobically expressed locus *aeg-46.5*. *J. Bacteriol.* **175**:1165–1172.
13. Cole, J. 1996. Nitrate reduction to ammonia by enteric bacteria: redundancy, or a strategy for survival during oxygen starvation? *FEMS Microbiol. Lett.* **136**:1–11.

14. **Craske, A., and S. J. Ferguson.** 1986. The respiratory nitrate reductase from *Paracoccus denitrificans*. Molecular characterisation and kinetic properties. *Eur. J. Biochem.* **158**:429–436.
15. **Darwin, A. J., and V. Stewart.** 1996. The NAR modulon systems: nitrate and nitrite regulation of anaerobic gene expression, p. 343–359. In E. C. C. Lin and A. S. Lynch (ed.), Regulation of gene expression in *Escherichia coli*. R. G. Landes Co., Georgetown, Tex.
16. **Darwin, A. J., and V. Stewart.** 1995. Nitrate and nitrite regulation of the Fnr-dependent *aeg-46.5* promoter of *Escherichia coli* K-12 is mediated by competition between homologous response regulators (NarL and NarP) for a common DNA-binding site. *J. Mol. Biol.* **251**:15–29.
17. **Darwin, A. J., K. L. Tyson, S. J. W. Busby, and V. Stewart.** 1997. Differential regulation by the homologous response regulators NarL and NarP of *Escherichia coli* K-12 depends on DNA binding site arrangement. *Mol. Microbiol.* **25**:583–595.
18. **Darwin, A. J., E. C. Ziegelhoffer, P. J. Kiley, and V. Stewart.** 1998. Fnr, NarP, and NarL regulation of *Escherichia coli* K-12 *napF* (periplasmic nitrate reductase) operon transcription in vitro. *J. Bacteriol.* **180**:4192–4198.
19. **DeMoss, J. A., and P. Y. Hsu.** 1991. NarK enhances nitrate uptake and nitrite excretion in *Escherichia coli*. *J. Bacteriol.* **173**:3303–3310.
20. **Fellay, R., J. Frey, and H. Krisch.** 1987. Interposon mutagenesis of soil and water bacteria: a family of DNA fragments designed for in vitro insertional mutagenesis of Gram-negative bacteria. *Gene* **52**:147–154.
21. **Gennis, R. B., and V. Stewart.** 1996. Respiration, p. 217–261. In F. C. Neidhardt, R. Curtiss III, J. L. Ingraham, E. C. C. Lin, K. B. Low, B. Magasanik, W. S. Reznikoff, M. Riley, M. Schaechter, and H. E. Umbarger (ed.), *Escherichia coli* and *Salmonella*. Cellular and molecular biology, 2nd ed. ASM Press, Washington, D.C.
22. **Goldman, B. S., and R. G. Kranz.** 2001. ABC transporters associated with cytochrome *c* biogenesis. *Res. Microbiol.* **152**:323–329.
23. **Grove, J., S. Busby, and J. Cole.** 1996. The role of the genes *nfEFG* and *cmfH* in cytochrome *c* biosynthesis in *Escherichia coli*. *Mol. Gen. Genet.* **252**:332–341.
24. **Grove, J., S. Tanapongpipat, G. Thomas, L. Griffiths, H. Crooke, and J. Cole.** 1996. *Escherichia coli* K-12 genes essential for the synthesis of *c*-type cytochromes and a third nitrate reductase located in the periplasm. *Mol. Microbiol.* **19**:467–481.
25. **Itoh, T., H. Aiba, T. Baba, K. Fujita, K. Hayashi, T. Inada, K. Isono, H. Kasai, S. Kimura, M. Kitakawa, M. Kitagawa, K. Makino, T. Miki, K. Mizobuchi, H. Mori, T. Mori, K. Motomura, S. Nakade, Y. Nakamura, H. Nashimoto, Y. Nishio, T. Oshima, N. Saito, G. Sampei, Y. Seki, S. Sivasundaram, H. Tagami, J. Takeda, K. Takemoto, C. Wada, Y. Yamamoto, and T. Horiuchi.** 1996. A 460-kb DNA sequence of the *Escherichia coli* K-12 genome corresponding to the 40.1–50.0 min region on the linkage map. *DNA Res.* **3**:379–392.
26. **Kepes, A.** 1969. Transcription and translation in the lactose operon of *Escherichia coli* studied by *in vivo* kinetics. *Prog. Biophys. Mol. Biol.* **19**:201–236.
27. **Kohara, Y., K. Akiyama, and K. Isono.** 1987. The physical map of the whole *E. coli* chromosome: application of a new strategy for rapid analysis and sorting of a large genomic library. *Cell* **50**:495–508.
28. **Kuritzkes, D. R., X.-Y. Zhang, and E. C. C. Lin.** 1984. Use of Φ (*glp-lac*) in studies of respiratory regulation of the *Escherichia coli* anaerobic *sn-glycerol-3-phosphate* dehydrogenase genes (*glpAB*). *J. Bacteriol.* **157**:591–598.
29. **Lin, J. T., and V. Stewart.** 1998. Nitrate assimilation by bacteria. *Adv. Microb. Physiol.* **38**:1–30.
30. **Liu, H. P., S. Takio, T. Satoh, and I. Yamamoto.** 1999. Involvement in denitrification of the *napKEFDABC* genes encoding the periplasmic nitrate reductase system in the denitrifying phototrophic bacterium *Rhodospirillum rubrum* f. sp. *denitrificans*. *Biosci. Biotechnol. Biochem.* **63**:530–536.
31. **MacGregor, C. H., C. A. Schnaitman, D. E. Normansell, and M. G. Hodgins.** 1974. Purification and properties of nitrate reductase from *Escherichia coli* K-12. *J. Biol. Chem.* **249**:5321–5327.
32. **Maloy, S. R., V. J. Stewart, and R. K. Taylor.** 1996. Genetic analysis of pathogenic bacteria. A laboratory manual. Cold Spring Harbor Laboratory Press, Cold Spring Harbor, N.Y.
33. **Metcalf, W. W., and B. L. Wanner.** 1993. Construction of new β -glucuronidase cassettes for making transcriptional fusions and their use with new methods for allele replacement. *Gene* **129**:17–25.
34. **Miller, J. H.** 1972. Experiments in molecular genetics. Cold Spring Harbor Laboratory, Cold Spring Harbor, N.Y.
35. **Monod, J., A. M. Pappenheimer, Jr., and G. Cohen-Bazire.** 1952. La cinétique de la biosynthèse de la β -galactosidase chez *Escherichia coli* considérée comme fonction de la croissance. *Biochim. Biophys. Acta* **9**:648–660.
36. **Moreno-Vivián, C., and S. J. Ferguson.** 1998. Definition and distinction between assimilatory, dissimilatory and respiratory pathways. *Mol. Microbiol.* **29**:664–666.
37. **Postma, P. W., and J. W. Lengeler.** 1985. Phosphoenolpyruvate:carbohydrate phosphotransferase system of bacteria. *Microbiol. Rev.* **49**:232–269.
38. **Potter, L., H. Angove, D. J. Richardson, and J. Cole.** 2001. Nitrate reduction in the periplasm of gram-negative bacteria. *Adv. Microb. Physiol.* **45**:51–112.
39. **Potter, L. C., P. Millington, L. Griffiths, G. H. Thomas, and J. A. Cole.** 1999. Competition between *Escherichia coli* strains expressing either a periplasmic or a membrane-bound nitrate reductase: does Nap confer a selective advantage during nitrate-limited growth? *Biochem J.* **344**:77–84.
40. **Potter, L. C., P. D. Millington, G. H. Thomas, R. A. Rothery, G. Giordano, and J. A. Cole.** 2000. Novel growth characteristics and high rates of nitrate reduction of an *Escherichia coli* strain, LCB2048, that expresses only a periplasmic nitrate reductase. *FEMS Microbiol. Lett.* **185**:51–57.
41. **Powell, B. S., M. P. Rivas, D. L. Court, Y. Nakamura, and C. L. Turnbough.** 1994. Rapid confirmation of single copy lambda prophage integration by PCR. *Nucleic Acids Res.* **22**:5765. (Erratum, **23**:1278, 1995.)
42. **Rabin, R. S., L. A. Collins, and V. Stewart.** 1992. *In vivo* requirement of integration host factor for nitrate reductase (*nar*) operon expression in *Escherichia coli* K-12. *Proc. Natl. Acad. Sci. USA* **89**:8701–8705.
43. **Rabin, R. S., and V. Stewart.** 1993. Dual response regulators (NarL and NarP) interact with dual sensors (NarX and NarQ) to control nitrate- and nitrite-regulated gene expression in *Escherichia coli* K-12. *J. Bacteriol.* **175**:3259–3268.
44. **Ralt, D., J. S. Wishnok, R. Fitts, and S. R. Tannenbaum.** 1988. Bacterial catalysis of nitrosation: involvement of the *nar* operon of *Escherichia coli*. *J. Bacteriol.* **170**:359–364.
45. **Richardson, D. J.** 2000. Bacterial respiration: a flexible process for a changing environment. *Microbiology* **146**:551–571.
46. **Richardson, D. J., and S. J. Ferguson.** 1992. The influence of carbon substrate on the activity of the periplasmic nitrate reductase in aerobically grown *Thiosphaera pantotropha*. *Arch. Microbiol.* **157**:535–537.
47. **Richardson, D. J., G. F. King, D. J. Kelly, A. G. McEwan, S. J. Ferguson, and J. B. Jackson.** 1988. The role of auxiliary oxidants in maintaining redox balance during phototrophic growth of *Rhodospirillum rubrum* on propionate or butyrate. *Arch. Microbiol.* **150**:131–137.
48. **Rowe, J. J., T. Ubbink-Kok, D. Molenaar, W. N. Konings, and A. J. M. Driessen.** 1994. NarK is a nitrite-extrusion system involved in anaerobic nitrate respiration by *Escherichia coli*. *Mol. Microbiol.* **12**:579–586.
49. **Sears, H. J., G. Sawers, B. C. Berks, S. J. Ferguson, and D. J. Richardson.** 2000. Control of periplasmic nitrate reductase gene expression (*napEDABC*) from *Paracoccus pantotrophus* in response to oxygen and carbon substrates. *Microbiology* **146**:2977–2985.
50. **Simons, R. W., F. Houtman, and N. Kleckner.** 1987. Improved single and multicopy *lac*-based cloning vectors for protein and operon fusions. *Gene* **53**:85–96.
51. **Skorupski, K., and R. K. Taylor.** 1996. Positive selection vectors for allelic exchange. *Gene* **169**:47–52.
52. **Stewart, G. S. A. B., S. Lubinsky-Mink, C. G. Jackson, A. Kassel, and J. Kuhn.** 1986. pHG165: a pBR322 copy number derivative of pUC8 for cloning and expression. *Plasmid* **15**:172–181.
53. **Stewart, V.** 1988. Nitrate respiration in relation to facultative metabolism in enterobacteria. *Microbiol. Rev.* **52**:190–232.
54. **Stewart, V.** 1982. Requirement of Fnr and NarL functions for nitrate reductase expression in *Escherichia coli* K-12. *J. Bacteriol.* **151**:1320–1325.
55. **Stewart, V., and C. H. MacGregor.** 1982. Nitrate reductase in *Escherichia coli*: involvement of *chlC*, *chlE*, and *chlG* loci. *J. Bacteriol.* **151**:788–799.
56. **Stewart, V., and J. Parales, Jr.** 1988. Identification and expression of genes *narL* and *narX* of the *nar* (nitrate reductase) locus in *Escherichia coli* K-12. *J. Bacteriol.* **170**:1589–1597.
57. **Stewart, V., and R. S. Rabin.** 1995. Dual sensors and dual response regulators interact to control nitrate- and nitrite-responsive gene expression in *Escherichia coli*, p. 233–252. In J. A. Hoch and T. J. Silhavy (ed.), Two-component signal transduction. ASM Press, Washington, D.C.
58. **Stewart, V., and C. Yanofsky.** 1986. Role of leader peptide synthesis in tryptophanase operon expression in *Escherichia coli* K-12. *J. Bacteriol.* **167**:383–386.
59. **Tanapongpipat, S., E. Reid, J. A. Cole, and H. Crooke.** 1998. Transcriptional control and essential roles of the *Escherichia coli* *ccm* gene products in formate-dependent nitrite reduction and cytochrome *c* synthesis. *Biochem. J.* **334**:355–365.
60. **Thomas, G., L. Potter, and J. A. Cole.** 1999. The periplasmic nitrate reductase from *Escherichia coli*: a heterodimeric molybdoprotein with a double-arginine signal sequence and an unusual leader peptide cleavage site. *FEMS Microbiol. Lett.* **174**:167–171.
61. **Thöny-Meyer, L.** 2000. Haem-polypeptide interactions during cytochrome *c* maturation. *Biochim. Biophys. Acta* **1459**:316–324.
62. **Tomsett, A. B., and R. H. Garrett.** 1980. The isolation and characterization of mutants defective in nitrate assimilation in *Neurospora crassa*. *Genetics* **95**:649–660.
63. **Tran, Q. H., J. Bongaerts, D. Vlad, and G. Unden.** 1997. Requirement for the proton-pumping NADH dehydrogenase I of *Escherichia coli* in respiration of NADH to fumarate and its bioenergetic implications. *Eur. J. Biochem.* **244**:155–160.
64. **Tyson, K. L., J. A. Cole, and S. J. W. Busby.** 1994. Nitrite and nitrate regulation at the promoters of two *Escherichia coli* operons encoding nitrite reductase: identification of common target heptamers for both NarP- and NarL-dependent regulation. *Mol. Microbiol.* **13**:1045–1055.
65. **Unden, G., and J. Bongaerts.** 1997. Alternative respiratory pathways of

- Escherichia coli*: energetics and transcriptional regulation in response to electron acceptors. *Biochim. Biophys. Acta* **1320**:217–234.
66. **Vieira, J., and J. Messing.** 1982. The pUC plasmids, an M13mp7-derived system for insertion mutagenesis and sequencing with synthetic universal primers. *Gene* **19**:259–268.
 67. **Wang, H., and R. P. Gunsalus.** 2000. The *nrfA* and *nirB* nitrite reductase operons in *Escherichia coli* are expressed differently in response to nitrate than to nitrite. *J. Bacteriol.* **182**:5813–5822.
 68. **Wang, H., C.-P. Tseng, and R. P. Gunsalus.** 1999. The *napF* and *narG* nitrate reductase operons in *Escherichia coli* are differentially expressed in response to submicromolar concentrations of nitrate but not nitrite. *J. Bacteriol.* **181**:5303–5308.
 69. **Winans, S. C., S. J. Elledge, J. H. Krueger, and G. C. Walker.** 1985. Site-directed insertion and deletion mutagenesis with cloned fragments in *Escherichia coli*. *J. Bacteriol.* **161**:1219–1221.
 70. **Wu, Q., and V. Stewart.** 1998. NasFED proteins mediate assimilatory nitrate and nitrite transport in *Klebsiella oxytoca (pneumoniae)* M5al. *J. Bacteriol.* **180**:1311–1322.